JPEDAV (2006) 27:231-244
DOI: 10.1361/154770306X109782
1547-7037/$19.00 ©ASM International

Computational Thermodynamic Model for the Mg-Al-Y System

S. Al Shakhshir and M. Medraj

(Submitted October 15, 2005; in revised form November 16, 2005)

The ternary Mg-Al-Y system was thermodynamically modeled based on the optimization of the binary subsystems Mg-Al, Mg-Y, and Al-Y using the CALPHAD approach. Mg-Al data was taken from the COST507 database, whereas the other two binary systems were reoptimized in this work. The liquid phase was described by a Redlich-Kister polynomial model, and the intermediate solid solutions were described by a sublattice model. Ternary interaction parameters were introduced to enable the best representation of the experimental data while considering the occurrence of the ternary compound Al_4MgY. The constructed database is used to calculate and predict thermodynamic properties, binary phase diagrams of Al-Y and Mg-Y, and liquidus projections of the ternary Mg-Al-Y. The calculated phase diagrams and the thermodynamic properties are in good agreement with the corresponding experimental data from the literature. Sixteen ternary four-phase-equilibria invariant points were predicted in the Mg-Al-Y system: seven ternary eutectic points, eight ternary quasi peritectic points, and one ternary peritectic point. Further, fifteen three-phase-equilibria invariant points were determined: eight saddle points and seven binary eutectic points.

Keywords Al-Y system, Al_4MgY, compound, Mg-Al based alloys, Mg-Al-Y phase diagram, Mg-Y system, thermodynamic modeling

1. Introduction

Magnesium alloys have been selected as candidates for automotive, aerospace, and aircraft applications because they are the lightest structural materials when compared with aluminum and iron.[1] Adding yttrium or rare-earth elements is one possible efficient method to improve the mechanical properties of Mg-Al-based alloys because it increases the corrosion, creep, and ignition resistance.[2-6] Precipitation of intermetallic or solid solution phases by Y addition to Mg-Al alloys is the reason behind improving the mechanical properties.[2,3] Therefore a complete knowledge of the phase diagram and thermodynamics of the ternary Mg-Al-Y system is essential for a better understanding of this system.

The Mg-Al-Y system has not been studied in its entirety. The goal of this work is to establish a complete thermodynamic description of this ternary system, which should in turn contribute to the effort of building a multicomponent thermodynamic database for Mg alloys. The resulting database will not only enable the calculation of the Mg-Al-Y phase diagram, but also will make possible the tracking of individual alloys, during heat treatment or solidification by calculation of phase distributions and phase compositions. This clearly will enable a better understanding of the Mg-Al-Y alloys and thus alloy development of new ones. To create an accurate thermodynamic model of a ternary system, it is necessary first to have thermodynamic descriptions of the three constituent binaries. Al-Y and Mg-Y systems were reoptimized in this work, and Mg-Al was taken from COST507.[7] A CALPHAD approach was used to build the Mg-Al-Y database. The reliability of the developed database is verified by comparison with the experimental data from the literature.

S. Al Shakhshir and **M. Medraj,** Department of Mechanical and Industrial Engineering, Concordia University, 1455 de Maisonneuve Blvd. West, Montreal, QC, H3G 1M8 Canada. Contact e-mail: mmedraj@encs.concordia.ca.

2. Analytical Description of the Thermodynamic Models Used

2.1 Unary Phases

The Gibbs energy function ${}^0G_i^\phi(T) = G_i^\phi(T) - H_i^{SER}$, used for the elements i (i = Al, Mg, and Y) in the phase ϕ is:

$${}^0G_i^\phi(T) = a + bT + cT\ln T + dT^2 + eT^3 + fT^{-1} + gT^7 + hT^{-9} \quad \text{(Eq 1)}$$

where ${}^0G_i^\phi(T)$ represents the Gibbs energy of the pure element, $G_i^\phi(T)$ is the Gibbs energy of the pure element in its standard state, H_i^{SER} [the molar enthalpy of the stable element reference (SER)] is at 25 °C and 1 atm, and T is the absolute temperature. The values of the coefficients a to h are taken from the SGTE compilation of Dinsdale.[8]

2.2 Stoichiometric Phases

The Gibbs energy of binary stoichiometric phases is:

$$G^\phi = x_i^0 G_i^{\phi 1} + x_j^0 G_j^{\phi 2} + \Delta G_f \quad \text{(Eq 2)}$$

where x_i and x_j are mol fractions of elements i and j, which are given by the stoichiometry of the compound, ${}^0G_i^{\phi 1}$ and ${}^0G_j^{\phi 2}$ are the respective reference states of elements i and j, and ΔG_f is the Gibbs energy of formation per mol of atoms of the stoichiometric compound:

$$\Delta G_f = a + bT \quad \text{(Eq 3)}$$

The parameters a and b are obtained by optimization using both the phase equilibria and thermodynamic data.

2.3 Disordered Solution Phases

The Gibbs energy of a disordered solution phase is:

$$G^{\phi} = x_i^0 G_i^{\phi} + x_j^0 G_j^{\phi} + RT[x_i \ln x_i + x_j \ln x_j] + {}^{ex}G^{\phi} \quad \text{(Eq 4)}$$

where ϕ denotes the phase of interest and x_i, x_j denote the mol fraction of component i and j, respectively. The first two terms on the right hand side of Eq 4 represent the Gibbs energy of the mechanical mixture of the components, the third term is the ideal Gibbs energy of mixing, and the fourth term is the excess Gibbs energy, which is described by a Redlich-Kister polynomial[9] in this work:

$${}^{ex}G^{\phi} = x_i . x_j \sum_{n=0}^{n=m} {}^nL_{i,j}^{\phi}(x_i - x_j)^n \quad \text{(Eq 5)}$$

$${}^nL_{i,j}^{\phi} = a_n + b_n \times T \quad \text{(Eq 6)}$$

where a_n and b_n are model parameters to be optimized in terms of experimental equilibrium and thermodynamic data.

2.4 Solid Solution Phases

The Gibbs energy of an ordered solution phase is:

$$G = G^{ref} + G^{ideal} + G^{excess} \quad \text{(Eq 7)}$$

$$G^{ref} = \sum y_i^l y_j^m \ldots . y_k^q \, {}^0G_{i:j:\ldots k} \quad \text{(Eq 8)}$$

$$G^{ideal} = RT \sum_l f_l \sum_i y_i^l \ln y_i^l \quad \text{(Eq 9)}$$

$$G^{excess} = \sum y_i^l y_j^l y_k^m \sum_{\gamma=0} {}^{\gamma}L_{(i,j):K} \times (y_i^l - y_j^l)^{\gamma} \quad \text{(Eq 10)}$$

where $i, j, \ldots k$ represent components or vacancy. l, m, and q represent sublattices. y_i^l is the site fraction of component i on sublattice l. f_l is the fraction of sublattice l relative to the total lattice sites. ${}^0G_{(i:j:\ldots k)}$ represents real or hypothetical compound energy. $L_{(i,j)}$ represent the interaction parameters that describe the interaction within the sublattice.

This general compound energy formalism (CEF) was used to describe the binary solid solutions $\gamma^{Mg\text{-}Y}$, δ, and ε in the Mg-Y binary system, and the ternary solid solution Al_4MgY (τ) in the ternary Mg-Al-Y system using the PANDAT package.[10] The ${}^0G_{(i:j:\ldots k)}$ and $L_{(i,j)}$ parameters of τ were adjusted by trial and error to fit the experimental data obtained by Odinaev and Ganiev.[11]

3. Experimental Data Evaluation

The first step of thermodynamic modeling and optimization is collecting and classifying the experimental data from the literature. Basically any type of experimental data pertinent to Gibbs energy can be used as an input for the thermodynamic modeling and optimization process. Typically, experimental phase diagram and thermochemical (e.g., enthalpy of mixing, activity, etc.) results are the data used for this purpose and can be collected from the literature.[12] Crystallographic data are also used because they are essential for Gibbs energy modeling of the long range ordered phases. The crystallographic information is mainly used for deciding the number of sublattices and the type of species that should be assigned on these sublattices, as will be discussed later. The second step is categorized under critical evaluation of the collected data. This evaluation eliminates the inconsistent and the contradictory experimental data.

3.1 Al-Y Binary System

3.1.1 Al-Y Phase Diagram Data. Savitiskii *et al.*[13] were the first to investigate the Al-Y system using metallographic and thermoanalytical measurements. They reported the formation of the peritectic intermetallic compound Y_2Al_5 at 1355 °C. A second compound was noticed and it was designated as Y_yAl_x. Snyder[14] studied the Al-Y system by thermal analysis, x-ray diffraction (XRD), and metallographic analyses. He reported, with ±5 °C accuracy, the liquidus, two congruent compounds Al_2Y and Al_2Y_3, which melt at 1485 and 1100 °C, respectively, and three incongruent melting compounds Al_3Y, AlY, and AlY_2. In this work, it was found that the eutectic reactions in the Al-rich and Y-rich regions take place at 640 and 960 °C, respectively. Further, the eutectic reaction L $\leftrightarrow$ Al_2Y_3 + AlY takes place at 1088 °C. The peritectic reactions for Al_3Y, Al_2Y, and AlY_2 take place at 980, 1130, and 985 °C, respectively. Lundin et al.[15] investigated this system by microstructural observations and x-ray methods and reported a phase diagram. Their results are in general agreement with Snyder[14] except in the following points: the solid solubility of Y in Al was less than 0.1 wt.% at the eutectic temperature and the YAl_3 peritectic reaction takes place at 1355 °C instead of 980 °C as reported by Snyder,[14] knowing that the accuracy of the reported temperature by Lundin et al.[15] was ±10 °C. Drits et al.[16] investigated the Al-rich region using thermal analysis and microstructural studies. Their results were also in good agreement with Snyder[14] and Lundin et al.[15] Further, Gschneidner et al.[17] assessed the Al-Y phase diagram based on the work of Lundin et al.[15] and Snyder.[14] They reported that βY phase melts at 1522 °C and yttrium undergoes an $\alpha \leftrightarrow \beta$ allotropic phase transformation at 1478 °C. Kripyakevich studied the Y-Al system by thermal analysis and reported the existence of another intermetallic compound Al_4Y.[18] However, Rongzhen et al.[19] found

that this compound does not exist in the Al-Y binary system when they investigated the Al-Y-Sn isothermal section at room temperature by XRD, differential thermal analysis (DTA), optical microscopy (OM), electron microscopy (SEM/EDS), electron spectrum and electron probe microanalysis (EPMA) techniques. Lingmin et al.[20] investigated the isothermal section of Al-Y-Sb at 527 °C by XRD with the aid of DTA, OM, and SEM. They confirmed the existence of Al_3Y, Al_2Y, AlY, Al_2Y_3, and AlY_3. They reported AlY_3 instead of AlY_2, which contradicts Snyder,[14] Lundin et al.,[15] and Rongzhen et al.[19] On the other hand, Chelkowsski et al.[21] found that the maximum solubility of Y in solid (Al) was less than 100 ppm using electrical and magnetic measurements and x-ray tests. Saveteskii et al.[13] found that the solubility of Y in Al is approximately 0.8 at.% Y at the eutectic temperature, and it was estimated to be less than 0.035 at.% Y at 300 °C. Richter et al.[22] identified the Y_5Al_3 compound as a $D8_8$ structure with Mn_5Si_3 prototype using transmission electron microscopy (TEM) and XRD. They reported that Y_5Al_3 is a metastable compound and should not appear in the phase diagram. A transformation of Al_3Y from α to β was noticed by Bailey[23] at 645 °C; however, the two different phases α and β were not confirmed by Raggio et al.,[24] or by Lingmin et al.[20]

3.1.2 Thermodynamic Data. The heat of mixing and the partial enthalpies were measured by Esin et al.[25] and Ryss et al.[26] calorimetrically at 1600 °C. The values reported in these two articles show a discrepancy, although they have common coauthors. This is caused by the difficulty in dealing with the Al-Y system experimentally because the reaction becomes more exothermic with adding yttrium. The partial Gibbs energy of yttrium was measured by Kobber et al.[27] at 527 °C using the electromotive force (emf) method. However, it was reported that the composition was not known for certain measured values of the partial Gibbs free energy in the range between 33 and 50% Y. Partial Gibbs energies and the heat of mixing were determined by Zviadadze et al.[28] using the vapor pressure technique. Their results show a discrepancy with the measurements of Esin et al.[25] and Ryss et al.[26] In this work, the experimental data of the partial Gibbs energy were not used in the optimization process because the results from the literature are contradictory and some compositions were not determined.

The heats of formation of Al_3Y, Al_2Y, and AlY were determined calorimetrically by Snyder,[14] Gröbner et al.,[29] and Timofeev et al.,[30] whereas Bronze et al.[31] used an emf method to measure the heat of formation of the AlY and Al_2Y compounds.

Kobber et al.[27] determined the activities of Al at 527 °C using the EMF technique. Petrusheveskii and Ryss[32] reported the activity of Al and Y at 1600 °C using the values obtained for heat of mixing by Ryss et al.,[26] whereas Kulifeev et al.[33] obtained the activities by measuring the partial vapor pressures of Al above Al-Y solid alloys.

The experimental results for the phase diagram obtained by Snyder[14] and Gscheidner et al.[17] were used in the optimization of the Al-Y system, because they are consistent with each other. However, the experimental data of Lundin et al.[15] were not used, due to the high error range in the reported temperature. Moreover, the heat of mixing obtained by Esin et al.[25] was used in the optimization process of this system because it was consistent with the other thermodynamic data such as the activities reported by Petrusheveskii and Ryss.[32] These experimental data were enough to optimize the model parameters of the system.

Table 1 Homogeneity ranges of the ε, δ, and $\gamma^{Mg\text{-}Y}$ phases

Phase	Temperature range, °C	Range of homogeneity, at.%Y	Reference
$\gamma^{Mg\text{-}Y}$, MgY	<935	48-50	38
ε, $Mg_{24}Y_5$	<605	13-16	38
δ, Mg_2Y	<780	33.2-34.2	39

3.2 Mg-Y Binary System

3.2.1 Mg-Y Phase Diagram. Sviderskaya and Padezhnova[34] used thermal analysis to study the Mg-rich region in Mg-Y alloys. A solid solution of Y in Mg was predicted and they noticed the existence of the $Mg_{24}Y_5$ compound in the Mg rich region. Gibson and Carlson[35] investigated the Mg-Y system using thermal, microscopic, and x-ray techniques. Their work accorded with Sviderskaya and Padezhnova.[34] Three compounds; $Mg_{24}Y_5$, Mg_2Y, and MgY were formed peritectically at 60, 41, and 21.5 wt.% Mg and represented by ε, δ, and $\gamma^{Mg\text{-}Y}$, respectively. The decomposition temperatures had been measured as 605, 780, and 935 °C, respectively. A eutectic reaction was identified at 74 wt.% Mg and 567 °C, and a eutectoid reaction associated with an allotropic transformation in Y at 11 wt.% Mg and 775 °C. The maximum solid solubility of Y in Mg was around 9 wt.% Y at 567 °C. Mizer and Clark[36] investigated the Mg-rich region using thermal analysis and metallography. They found that the maximum solubility of Y in solid Mg was approximately 12.6 wt.% Y at the eutectic temperature 565.5 °C. This work shows good agreement with Sviderskaya and Padezhnova[34] and Gibson and Carlson.[35] Besides, Massalski[37] assessed the Mg-Y phase diagram using the experimental work in the literature and had to adjust his results to comply with the results of Sviderskaya and Padezhnova[34] in the Mg-rich region. Smith et al.[38] found using XRD that $Mg_{24}Y_5$ and MgY have tangible homogeneity ranges, as shown in Table 1. The Mg_2Y phase was predicted as intermetallic compound by Carlson,[35] Mizer and Clark,[36] and Smith et al.[38] These results do not agree with Flandorfer et al.[39] who used XRD, OM, and EPMA to study the Ce-Mg-Y isothermal section at 500 °C. From their experimental work, the range of homogeneity of the Mg_2Y was obtained, as shown in Table 1.

The crystal structures of δ, ε, and $\gamma^{Mg\text{-}Y}$ were investigated using XRD by Smith *et al.*[38] They reported that $\gamma^{Mg\text{-}Y}$ has CsCl structure, δ-phase has $MgZn_2$ structure, and ε-phase has α-Mn structure. Further, the crystal structure of ε was studied again in 2004 by Zhang et al.[40] using TEM. They reported the same crystal structure as found by Smith

et al.,[38] but with one difference in the occupying atoms of the 2a Wyckoff position. Zhang et al.[40] reported that this position was occupied by an Mg atom, however Smith et al.[38] reported that this position was occupied by 0.25 at.% Mg and 0.75 at.% Y. The work of Zhang et al. [40] is more precise than Smith et al.[38] because they used a much more advanced experimental technique for predicting the crystal structure. Therefore these results will be used in the current research. The crystallographic data will be discussed later under the modeling section of these phases.

3.2.2 Thermodynamic Data. Agrawal et al.[41] measured the enthalpy of mixing of liquid Mg-Y alloys in the Mg-rich region calorimetrically at different temperatures. The maximum composition attained was 21.8 at.%Y at 747 °C. Agrawal et al. extrapolated the values of the heat of mixing over the remaining composition range using the association model. Fabrichanya et al.[42] calculated the heat of mixing of Mg-Y liquid alloys. These calculations showed good agreement with Agrawal et al.[41] Activities of Mg and Y were measured by Gansen et al.[43] using the vapor pressure technique. These results are in agreement with the measured activities of Mg by Ipser and Gansen[44] using the same method. Both results are consistent with the activities calculated by Fabrichanya et al.[42]

Smith et al.[38] measured the enthalpies of formations using differential acid solution calorimetry and vapor pressure measurements. The heat of formation of $Mg_{24}Y_5$ was measured by Smith et al.[38] and found consistent with the calculated value by Ran et al.[45] However, the other intermediate compounds showed fair agreement between Smith et al.[38] and Ran et al.[45] This is caused by the difficulties in measuring the heat of formation when the Y content increases because the reactions become more exothermic. Also, Y has a high melting point compared with Mg, and this leads to sublimation of Mg during fusion of the metals.[41] Fabrichanya et al.[4] calculated the heat of formation, and their results showed a reasonable agreement with the one measured by Smith et al.[38] and with the experimental data obtained calorimetrically by Payagi et al.[46]

The experimental data for the Mg-Y phase diagram obtained by Sviderskaya and Padezhnova,[34] Massalski,[37] and Smith et al.[38] were quite enough to optimize the Mg-Y binary system. The experimental thermodynamic data were in agreement with the current calculations.

3.3 Mg-Al Binary System

The binary Mg-Al system has already been thermodynamically evaluated by COST507 project[7] in an effort to build a multicomponent Mg data base. In the current work, the Mg-Al system is taken from this database because it is in agreement with the experimental data in the literature, and the models used and the number of parameters for each phase are consistent with the current treatment of the other two binary systems.

This system has two terminal solid solutions, hcp-Mg and fcc-Al; two intermetallic compounds, $Al_{30}Mg_{23}$ and $Al_{140}Mg_{89}$; and a nonstoichiometric compound, $\gamma^{Mg\text{-}Al}$. The line compound $Al_{30}Mg_{23}$ is stable only in the temperature range of 250-410 °C. Two congruent melting compounds are identified: $\gamma^{Mg\text{-}Al}$ melts at 464 °C and $Al_{140}Mg_{89}$ melts at 452 °C. The first eutectic reaction is identified in the Mg-rich region at 30 at.% Mg and 435 °C, the second eutectic reaction is between $\gamma^{Mg\text{-}Al}$ and $Al_{140}Mg_{89}$ at 58 at.% Mg and 448 °C, and the third one is in the Al-rich region at 64 at.% Al and 450 °C.

3.4 Mg-Al-Y Ternary System

Drits et al.[47] investigated the Mg-Al-Y system using DTA, microscopy, and micro x-ray spectrum analysis. Their investigations showed that the ε, $\gamma^{Mg\text{-}Al}$, and Al_2Y are in equilibrium with hcp-Mg phase in four different regions in the phase diagram. Zarechnyuk et al.[48] studied this system experimentally in the range of 0-33 at.% Y at 400 °C using XRD, microstructure, and chemical analysis. They confirmed the results obtained by Drits et al.[47] Zarechnyuk et al.[48] detected for the first time the existence of a τ (Al_4MgY) ternary compound. This compound was in equilibrium with Al_3Y, Al_2Y, Al_3Mg_2, and fcc-Al in four different regions in the phase diagram. It was reported that the ternary Al_4MgY compound has the $MgZn_2$ crystal structure type. The crystallographic data will be addressed during the modeling process of this phase. Odinaev and Ganiev[11] used XRD, metallographic analysis, and DTA to construct the liquidus surfaces and to determine the characteristic points in the Al-Mg-Al_2Y section.[11] They confirmed the existence of the τ-phase detected by Zarechnyuk et al.[48] They reported the primary solidification region of τ-phase and showed that this phase melts congruently at 780 °C. Odinaev et al.[49] constructed the Mg-Al-Y isothermal section at 400 °C over the entire composition range using microstructural analysis and XRD. In this work, the existence of the τ-phase was confirmed. Also, the existences of extensive solid solubility between the intermetallic compounds were observed along 33.3 at.% and 50 at.% Y sections. It is worth mentioning that the existence of such extensive solid solutions was not observed by Zarechnyuk et al.[48] and Odinaev and Ganiev.[11] The results of Odinaev et al.[49] were not included in the current work because the phase boundaries in the composition range of 33.3-100 at.% Y were determined based on analogy with the phase equilibria in the Al-Mg-(La, Ce, Pr, and Nd) ternary systems.

4. Results and Discussion

4.1 Al-Y Binary System

In 1989, Ran et al.[50] calculated the Al-Y system. They used 5-Redlich-Kister polynomial terms for the liquid phase; however, the results did not agree with the experimental results of the integral heat of mixing and partial activities. In 1995, Gröbner et al.[29] reoptimized the system, also, with 5-Redlich-Kister polynomial terms for the liquid phase to be used in the extrapolation of Al-Y-C ternary system. In this work, the AlY compound was considered as a congruent melting compound; this disagrees with the experimental data from the literature.[14,15,19] Further, this model does not reproduce the experimental thermodynamic data reported in the literature except for the heats of formation of the intermetallic compounds. Thus, this system was reoptimized in the current work.

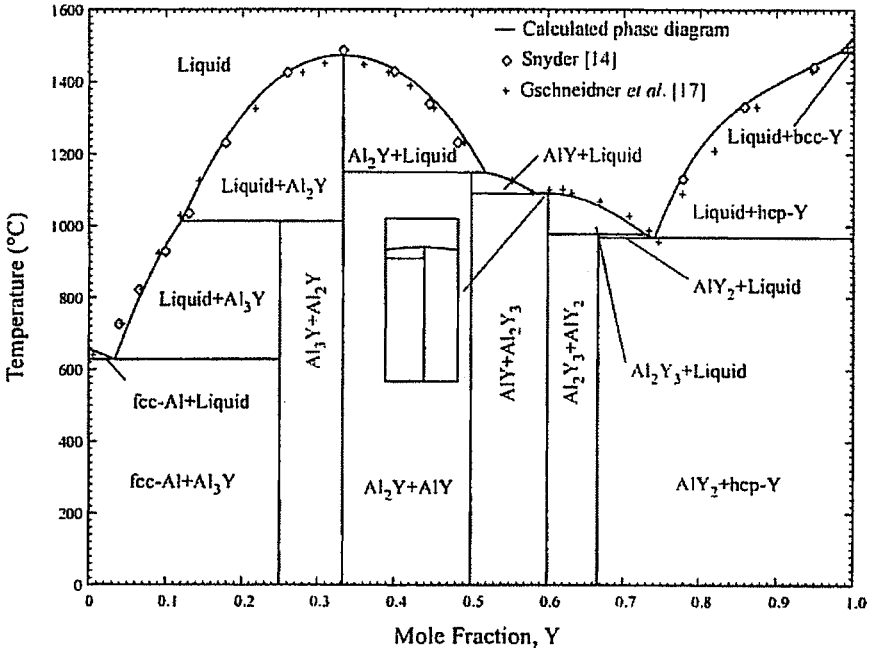

Fig. 1 Calculated Al-Y phase diagram with experimental results from the literature

Table 2 Optimized model parameters for the liquid and intermetallic compounds in the Al-Y system

Phase	Terms	*a*, J/mol	*b*, J/molK
Liquid	L_0	−160,876.360	5.000
	L_1	−32,000.000	7.560
	L_2	32,000.000	−6.530
Al_3Y	ΔG_f	−39,727.972	8.036
Al_2Y	ΔG_f	−50,410.046	10.230
AlY	ΔG_f	−48,074.303	11.536
Al_2Y_3	ΔG_f	−45,347.395	12.364
AlY_2	ΔG_f	−38,200.000	10.568

4.1.1 Phase Diagram. The selected experimental phase diagram and enthalpy of mixing of liquid Al-Y alloys, which were discussed in Sec. 3, were used to optimize the thermodynamic model parameters for all the phases in the Al-Y binary system. To maintain the consistency with other systems, and with the COST507 project,[7] no lattice stability values were added to the Gibbs energy expressions obtained from the SGTE database[8] for the pure components, cph-Mg, fcc-Al, cph-Y, and bcc-Y.

In the current work, the Al-Y system was optimized and calculated using three Redlich-Kister terms for the liquid, as shown in Table 2. In general, a simpler model with fewer parameters is preferred to the more complicated ones. The model-calculated phase diagram of the Al-Y system in relation to the experimental results from the literature is shown in Fig. 1. This figure shows good agreement with the published experimental data.

4.1.2 Thermodynamic Data. The calculated heat of mixing, shown in Fig. 2(a), illustrates good agreement with the experimental data obtained by Esin et al.[25] and Ryss et al.,[26] except in the 0.33-0.55 composition range where the experimental data shows a negative deviation from the calculated values; however, both have the minimum point at the same composition. This deviation is not only between the calculated and the experimental data; it can also be seen between the experimental results of Ryss et al.[25] and Esin et al.,[26] as shown in Fig. 2(a). This discrepancy is probably caused by the difficulty in obtaining accurate measurements in this region, due to the existence of the high melting Al_2Y compound (T_m = 1475 °C). However, the work of Zviadadze et al.[28] shows a large discrepancy with the current calculation as well as with the earlier work of Ryss et al.[25] and Esin et al.[26] This discrepancy is probably due to the fact that the vapor pressure experimental technique used by Zviadadze et al.[28] is less accurate than the calorimetric experimental technique used by the two earlier investigations.[25,26]

The calculated activities are shown in Fig. 2(b), where good agreement with Petrusheveskii and Ryss[32] can be observed. However, the activity measured by Kulfieev et al.[33] shows poor agreement with the current calculations. This is due to the systematic error, which is attributed to using different techniques in activity measurement.[51] The calculated partial heats of mixing of Al and Y show good agreement with other experimental data (Fig. 2c).[24,25] A slight positive deviation is noticed in the calculated data over the experimental results. Nonetheless, the trend is similar. However, the experimental partial heats of mixing of Al and Y obtained by Zviadadze et al.[28] show poorer agreement with the calculated partial heat of mixing and contradict other experimental work.[24,25]

Figure 2(d) shows good agreement between the calculated heats of formation obtained in this study and the experimental results[29,31] already reported. On the other hand, the heats of formation of Al_2Y, Al_3Y, and AlY measured by Snyder[14] are more negative than the calculated ones. This

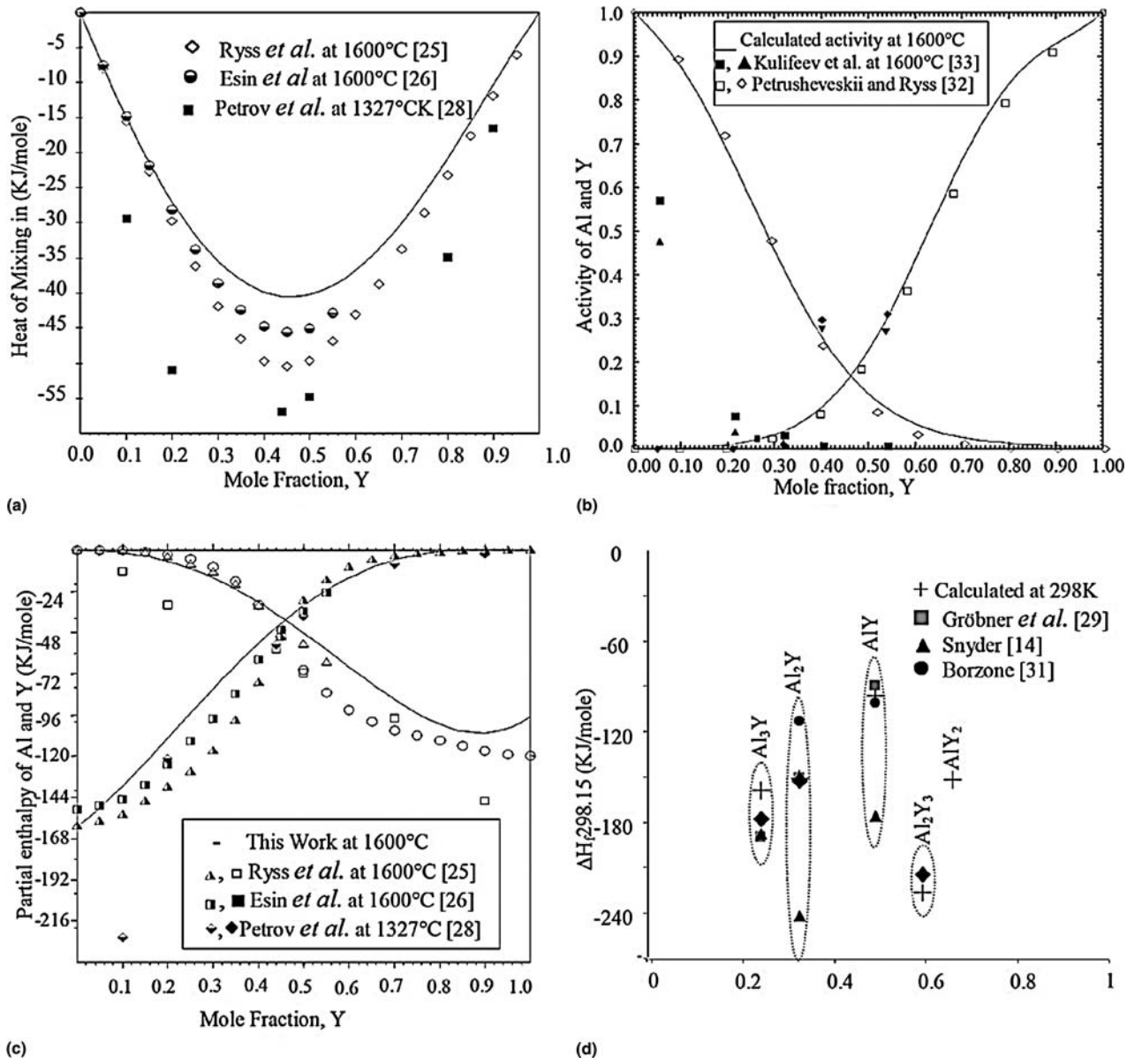

Fig. 2 Calculated thermodynamic properties of the Al-Y system compared with experimental data from the literature: (a) heat of mixing of Al-Y liquid, (b) activities of Al and Y, (c) partial enthalpy of mixing Al and Y, and (d) enthalpy of formation of the stoichiometric compounds

higher negativity is caused by employing the estimations of Miedema et al.[52] to calculate the heat of formations of the three intermetallic compounds in the work of Snyder.[14] The calculated heat of formation of the most stable intermetallic compound Al_2Y shows excellent agreement with the results of Baily[23] and Gröbner et al.,[29] as shown in Fig. 2(d).

4.2 Mg-Y Binary System

In 1988, Ran et al.[45] calculated the Mg-Y phase diagram using optimized parameters of phase equilibria and thermodynamic data. In this work, δ-phase was considered stoichiometric. However, Flandorfer et al.[39] had reported a range of homogeneity for this compound. The assessment of the thermodynamic data from the related literature such as the heat of mixing, activities, and partial Gibbs energy was not discussed by Ran et al.[45] In 2003, Fabrichanya et al.[42] recalculated the Mg-Y system using both phase equilibria and thermodynamic data in the optimization process. They used a sublattice model, and they reproduced the homogeneity ranges of ε, δ, and $\gamma^{Mg\text{-}Y}$. Their calculations showed good agreement with the phase diagram and the thermodynamic data from the related literature. Although they reproduced the homogeneity ranges of ε, δ, and $\gamma^{Mg\text{-}Y}$ phases in their calculation, they did not consider the crystallographic data for ε, δ, and $\gamma^{Mg\text{-}Y}$ phases in the modeling process. Besides, they modeled the $\gamma^{Mg\text{-}Y}$ phase using at least 10 parameters that can result in unpredictable calculations for the higher order systems. Therefore, this system was re-optimized in the current work.

Table 3 Optimized Redlich-Kister model parameters for all the phases in Mg-Y system

Phase	Terms	*a*, J/mol	*b*, J/molK
Liquid	L_0	−40,917.970	22.830
	L_1	−18,685.230	10.240
	L_2	1,076.670	−6.050
Hcp-Mg	L_0	−11,718.260	7.490
	L_1	−4,305.600	2.430
	L_2	−7,236.360	2.000
β-Y	L_0	−28,199.320	13.490
	L_1	−2,005.000	1.500
ε, $Mg_{24}Y_5$	G (Mg:Mg:Mg)	48.930	0.000
	G (Mg:Y:Mg)	−208.621	0.000
	G (Y:Y:Mg)	206.900	−0.103
δ, Mg_2Y	G (Mg:Mg:Mg)	600.000	0.000
	G (Mg:Y:Mg)	−2,956.667	−0.017
	G (Y:Y:Mg)	1,333.333	0.000
	G (Y:Mg:Mg)	−1,666.667	54.340
	L (Mg, Y:Mg:Mg; 0)	−5,000.000	336.160
	L (Mg, Y:Y:Mg; 0)	−7,816.920	20.440
	L (Mg:Mg, Y:Mg; 0)	−3,910.068	3.470
	L (Y:Mg, Y:Mg; 0)	−5,000.000	336.440
$\gamma^{Mg\text{-}Y}$, MgY	G (Mg:Y)	−9,675.000	1.210
	G (Mg:Va)	5,000.000	0.000
	G (Y:Y)	−2,895.780	10.750
	G (Y:Va)	13,500.000	17.500
	L (Mg, Y:Y; 0)	15,000.000	16.000
	L (Mg, Y:Va; 0)	15,000.000	15.000
	L (Mg:Y, Va; 0)	−5,000.000	7.000
	L (Y:Y, Va; 0)	−5,000.000	7.000

4.2.1 Phase Diagram. In the current work, the Mg-Y system was reoptimized using the experimental phase equilibria data and employing a Redlich-Kister description of the liquid, hcp-Mg, and β-Y phases, and the general compound energy formalism (CEF) or sublattice model for the ε, δ, and $\gamma^{Mg\text{-}Y}$ phases (Table 3).

The calculated phase diagram shows good agreement with the experimental data from the literature (Fig. 3). This figure shows that the calculated ranges of homogeneities are also consistent with experimental data.

4.2.2 Thermodynamic Modeling of the ε, δ, and $\gamma^{Mg\text{-}Y}$ Phases. As a first approximation of the Mg-Y system, the ε, δ, and $\gamma^{Mg\text{-}Y}$ phases were modeled as linear compounds using the stoichiometric model. Once a satisfactory thermodynamic description of each phase, especially the liquid phase, was obtained, these phases were remodeled as solid solutions using the sublattice model. This was done gradually, starting with the highest melting temperature $\gamma^{Mg\text{-}Y}$ phase and ending with the lowest melting temperature ε-phase. This is because the highest melting temperature compound has more effect on the thermodynamic description of the other phases. Hari Kumar et al.[53] and Hari Kumar and Wollants[12] mentioned that attention should be given to the crystallographic information and the solubility range of the phase during the optimization of the sublattice model parameters.

Thermodynamic Modeling of the $\gamma^{Mg\text{-}Y}$ Phase. The crystal structure data of the $\gamma^{Mg\text{-}Y}$ intermediate solid solutions was obtained by Smith et al.[38] and listed in the Pearson handbook[54] (Table 4).

The coordination numbers shown in Table 4 were obtained in this work. The coordination number is defined as the number of closest neighbor similar and dissimilar atoms around the atom of interest.[53] This number is determined from the substructure of each atom drawn by the PowderCell software[55] using the available crystallographic data (Fig. 4).

Based on the crystallographic data of $\gamma^{Mg\text{-}Y}$ phase, there are two atoms at different sites in the unit cell with the same point of symmetry and different coordination number (Table 4). To obtain an intermediate phase that has an ideal stoichiometry, two sublattices are needed, and each sublattice is occupied by only one constituent species. In other words, the direct sublattice model based on the crystallographic data of the $\gamma^{Mg\text{-}Y}$ phase requires consideration of only two sublattices: one occupied by Mg and the other by Y.

$$(Mg)_1: (Y)_1$$

This model does not represent the homogeneity range of γ-phase obtained by Smith et al.[38] To achieve the deviation from stoichiometry, it is necessary to allow mixing of atoms in one or more sublattices. For the phases that have a relatively narrow range of homogeneity like $\gamma^{Mg\text{-}Y}$ the mixing is performed by "defects," which may be vacancies or antistructure atoms (i.e., atoms at lattice sites belonging to the other kind of atoms in the ideal structure).[12,53] Based on that, the mixing of Y atoms as antistructure atoms in Mg sublattice and vacancies (Va) in Y sublattice are the defects considered in this model. Therefore, the model takes the form:

$$(Mg\%, Y)_1: (Y\%: Va)_1$$

Here the % denotes the major constituent of the sublattice. This model covers the whole composition range. Therefore, this satisfies the homogeneity range requirement for $\gamma^{Mg\text{-}Y}$ phase obtained by Smith et al.[38] as $0.48 \le X_Y \le 0.5$. Thus, the Gibbs energy per mole of formula unit of MgY is given by Eq 11:

$$\begin{aligned} G_m^{MgY} &= y_{Mg}^{I} y_Y^{II\,0}G_{Mg:Y}^{MgY} + y_{Mg}^{I} y_{Va}^{II\,0}G_{Mg:Va}^{MgY} \\ &+ y_Y^{I} y_Y^{II\,0}G_{Y:Y}^{MgY} + y_Y^{I} y_{Va}^{II\,0}G_{Y:Va}^{MgY} \\ &+ RT\left(0.5\sum_{i=Mg}^{Y} y_i^{I}\ln y_i^{I} + 0.5\sum_{i=Y}^{Va} y_i^{II}\ln y_i^{II}\right) \\ &+ y_{Mg}^{I} y_Y^{I}\left(y_Y^{II\,0}L_{Mg,Y:Y}^{MgY} + y_{Va}^{II\,0}L_{Mg,Y:Va}^{MgY}\right) \\ &+ y_Y^{II} y_{Va}^{II}\left(y_{Mg}^{I\,0}L_{Mg:Y,Va}^{MgY} + y_Y^{I\,0}L_{Y:Y,Va}^{MgY}\right) \end{aligned} \quad \text{(Eq 11)}$$

where, i is the species inside the sublattice. y_{Mg}^{I}, y_Y^{I} is the site fraction of sublattice I. y_Y^{II}, y_{Va}^{II} is the site fractions of lattice II. ${}^0G_{Mg:Y}^{MgY}$, ${}^0G_{Mg:Va}^{MgY}$, ${}^0G_{Y:Y}^{MgY}$, ${}^0G_{Y:Va}^{MgY}$, ${}^0L_{Mg,Y:Y}^{MgY}$, ${}^0L_{Mg,Y:Va}^{MgY}$, ${}^0L_{Mg:Y,Va}^{MgY}$, and ${}^0L_{Y:Y,Va}^{MgY}$ are the model parameters that were optimized using the CEF with the experimental data shown in Table 3 using the PANDAT program.[10]

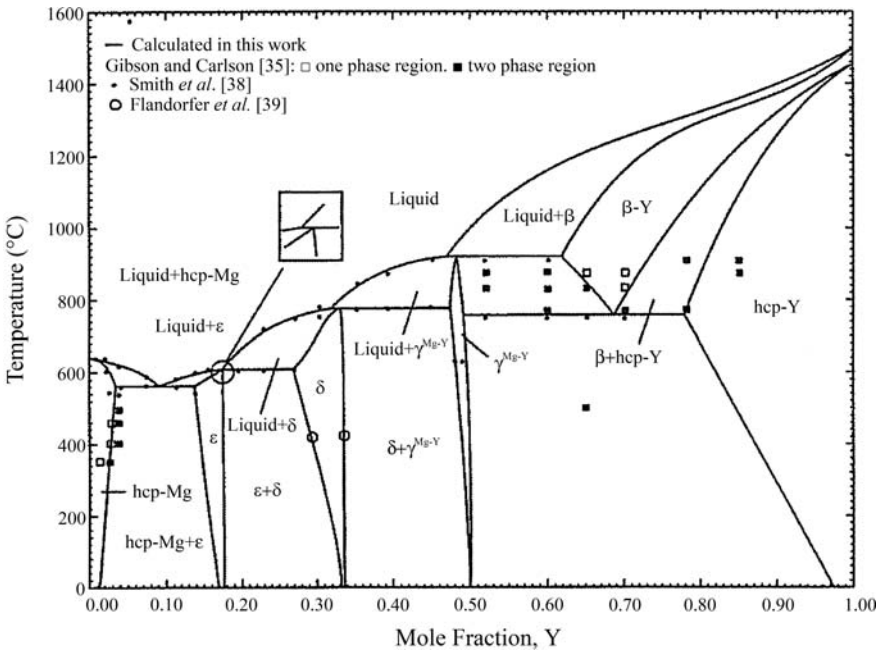

Fig. 3 Calculated Mg-Y phase diagram with experimental results from the literature

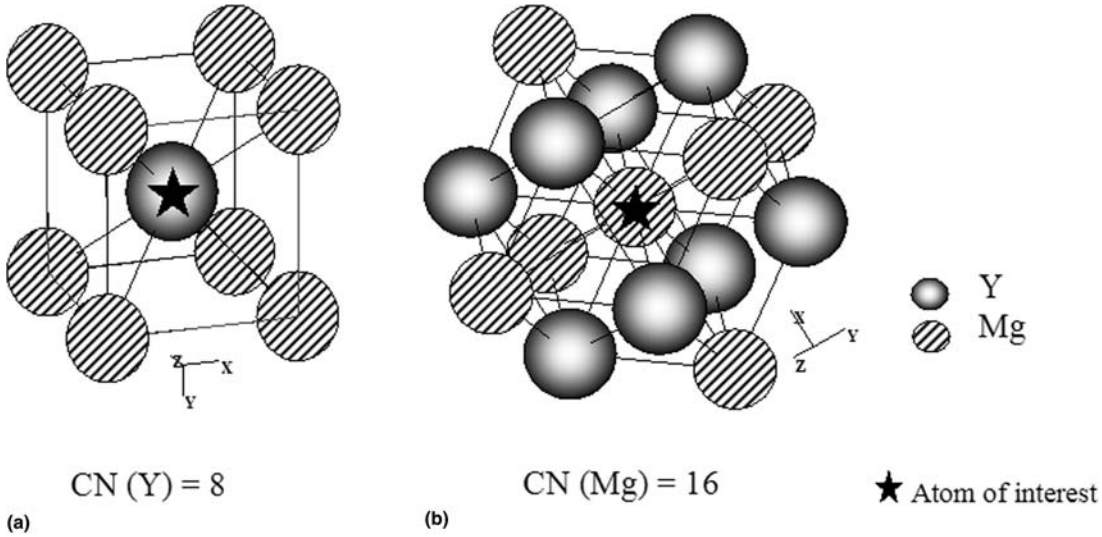

Fig. 4 Substructure of (a) Y and (b) Mg atoms in $\gamma^{Mg\text{-}Y}$ unit cell with the coordinator number (CN)

Table 4 Crystal structure and lattice parameters of $\gamma^{Mg\text{-}Y}$ phase

Phase	Crystal data	Atoms	WP(a)	CN(b)	PS(c)	Atomic position X	Y	Z
$\gamma^{Mg\text{-}Y}$, MgY	Structure type, C1Cs	Mg	1*a*	14	$m\bar{3}m$	0	0	0
	Pearson symbol, *cP*2	Y	1*b*	14	$m\bar{3}m$	½	½	½
	Space group, $Pm\bar{3}m$							
	Space group No., 221							
	Lattice parameter, nm, $a = 0.3810$							
	Angles: $\alpha = 90°$, $\beta = 90°$, $\gamma = 120°$							

(a) WP, Wyckoff position, (b) CN, coordination number, and (c) PS, point symmetry. Source: Ref 54

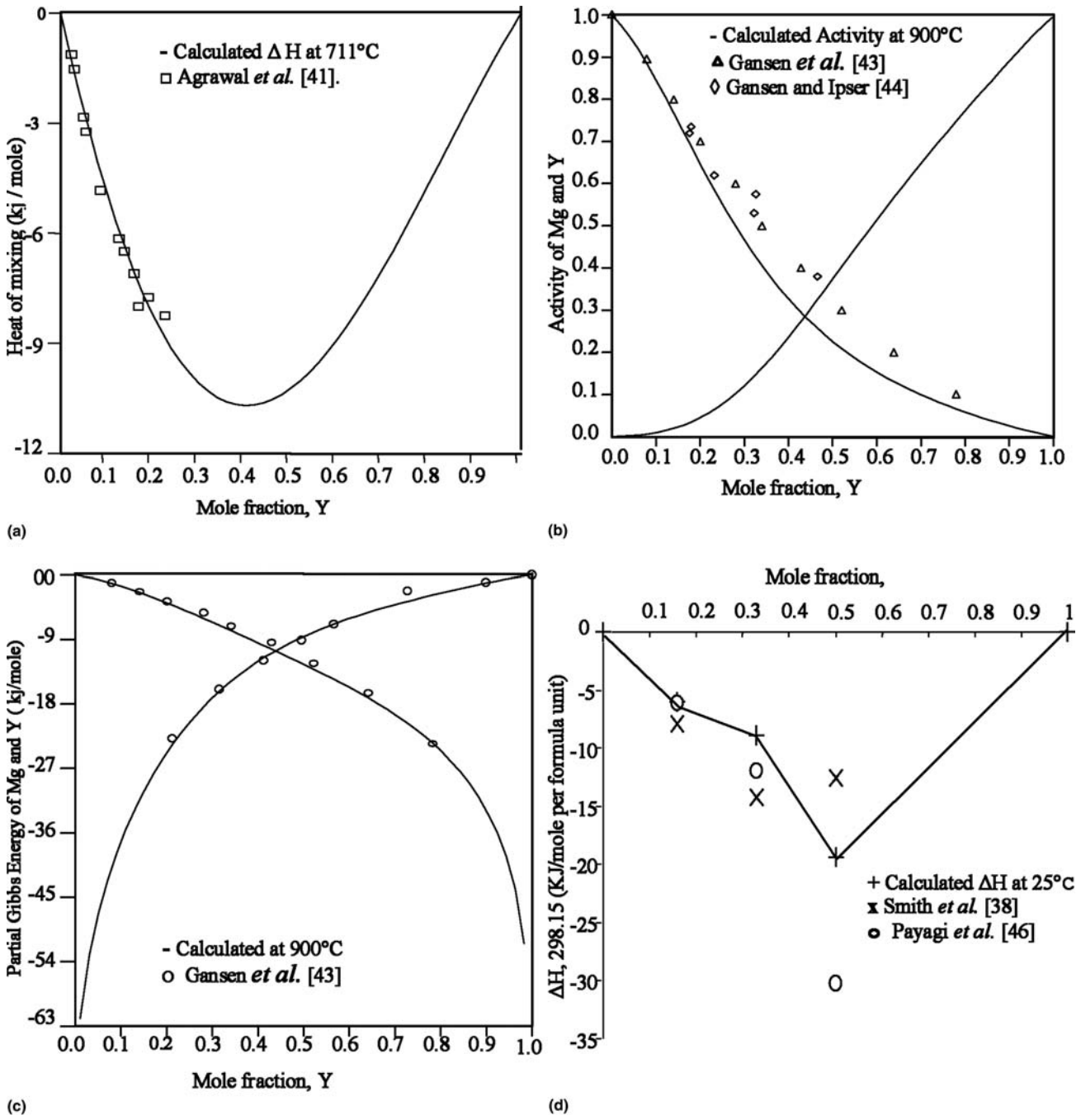

Fig. 5 Calculated thermodynamic properties compared with the experimental data from the literature: (a) heat of mixing of Mg-Y liquid, (b) activities of Mg and Y, (c) partial Gibbs energy of Mg and Y, and (d) enthalpy of formation of the stoichiometric compounds

Thermodynamic Modeling of the ε-Phase. The ε-phase was modeled in the same way as the $\gamma^{Mg\text{-}Y}$ phase.

$$(Mg\%, Y)_{29}: (Y\%, Mg)_{10}: (Mg)_{19}$$

the maximum homogeneity range of $0.13 \leq X_Y \leq 0.16$ at 545 °C reported by Smith et al.[38] is included by the range of this model that covers $0 \leq X_Y \leq 0.672$. Based on this model, an equation similar to that of $\gamma^{Mg\text{-}Y}$ can be established by taking into account the new number of sublattices and the new site fractions.

Thermodynamic Modeling of the δ-Phase. Similarly, the δ-phase was modeled and the resultant mode is:

$$(Mg\%, Y)_6: (Y\%, Mg)_4: (Mg)_2$$

This model covers the $0 \leq X_Y \leq 0.833$ composition range. This range includes the homogeneity range of $0.332 \leq X_Y$

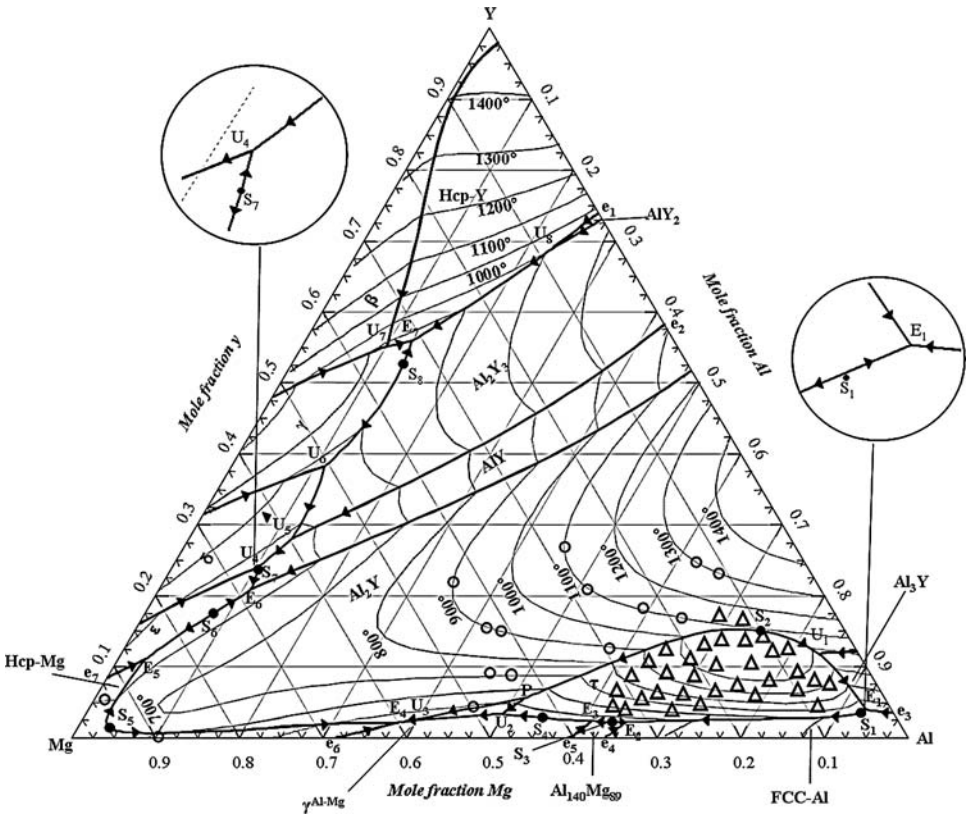

Fig. 6 Calculated Al-M-Y ternary phase diagram with invariant points: (○) experimental liquidus isotherms and (△) primary solidification region for τ-phase[11]

Table 5 Ternary interaction parameters with the τ-phase parameters

Terms	*a*, J/mol	*b*, J/molK
L_0 (Mg, Al, Y)	–150,000.000	0.000
L_1 (Mg, Al, Y)	–180,000.000	0.000
G (Al:Mg:Y)	–4,166.667	1.401
G (Al:Al:Y)	–3,500.000	0.883
G (Al:Y:Mg)	–4,333.333	0.733
L (Al, Mg, Y:Al:Mg;0)	–96,000.000	4.000

$\leq$ 0.342 reported by Flandorfer et al.[39] Based on the established number of sublattices and the site fractions, the δ-phase was modeled and the model parameters were optimized (Table 3).

4.2.3 Thermodynamic Properties of the Mg-Y System. Figure 5(a) shows that the calculated heat of mixing is in good agreement with the experimental results of Agrawal et al. [41] The calculated activity of Mg in Mg-Y liquid has a slight negative deviation from the experimental values reported by Zhang and Kelly[40] and Agrawal et al.[41] (Fig. 5b). The experimental values of Y activity are not available in the literature; therefore, comparison was not possible. The calculated partial Gibbs free energy of Mg and Y in Mg-Y liquid is in good agreement with the experimental results of Zarechnyuk et al.[48] (Fig. 5c). Figure 5(d) shows the calculated heat of formation of the intermediate compounds in the Mg-Y system in relation to experimental results from the literature. Good agreement between the calculated and the experimental data is noticed. The $\gamma^{Mg\text{-}Y}$ phase, reported by Pyagai et al.[46] has a negative value twice that in this work and that obtained by Smith et al.[38] The measurements of Smith et al.[38] were more accurate than those of Pyagai et al.[46] This is because Smith et al.[38] used both calorimetric and vapor pressure techniques that produced consistent results. However, Pyagai et al.[46] used the calorimetric technique only. The value obtained in the current work lies between these two results but closer to that of Smith et al.[38]

4.3 Mg-Al-Y System

A self-consistent thermodynamic database for the Mg-Al-Y system has been constructed by combining the thermodynamic descriptions of the three constituent binaries; Al-Y, Mg-Y, and Mg-Al, along with the thermodynamic properties of the ternary compound τ (Al_4MgY), which have been assessed in this work.

4.3.1 Thermodynamic Modeling of τ-phase. The ternary solid solution τ (Al_4MgY) was modeled using the CEF with the experimental data of the primary solidification region reported by Odinaev and Ganiev[11] using DTA. The sublattice model was determined in the same way as $\gamma^{Mg\text{-}Y}$. The resultant model for the τ-phase is:

Table 6 Calculated four-phase equilibria points and their reactions in the Al-Mg-Y system

No.	Reaction	Calculated invariant points				
				Composition, at.%		
		T, °C	Type	Al	Mg	Y
1	Liquid ↔ τ + Al_3Y + fcc-Al	612.8	E_1	93	3	4
2	Liquid ↔ fcc-Al + $Al_{140}Mg_{89}$ + τ	431.4	E_2	65.2	32.7	2.1
3	Liquid ↔ $Al_{140}Mg_{89}$ + τ + $\gamma^{Al\text{-}Mg}$	430.5	E_3	61	36.7	2.3
4	Liquid ↔ $\gamma^{Mg\text{-}Y}$ + Al_2Y + cph-Mg	419.6	E_4	37.6	60.4	2
5	Liquid ↔ Al_2Y + cph-Mg + ε	538.5	E_5	3.3	85.6	1.1
6	Liquid ↔ Al_2Y + ε + AlY	817.5	E_6	11	68	21
7	Liquid ↔ Al_2Y_3 + $\gamma^{Mg\text{-}Y}$ + cph-Y	727	E_7	12.7	31.4	55.9
8	Liquid + Al_2Y ↔ τ + Al_3Y	969.1	U_1	83.4	4.7	11.9
9	Liquid + τ ↔ $\gamma^{Mg\text{-}Y}$ + Al_3Y	434.6	U_2	50	47	3
10	Liquid + Al_3Y ↔ $\gamma^{Mg\text{-}Y}$ + Al_2Y	693.8	U_3	37.6	60.4	2
11	Liquid + δ ↔ ε + AlY	549.7	U_4	10.3	65.6	24.1
12	Liquid + Al_2Y_3 ↔ AlY + δ	575.3	U_5	12.3	59.6	28.1
13	Liquid + $\gamma^{Mg\text{-}Y}$ ↔ δ + Al_2Y_3	652	U_6	11	50.7	38.3
14	Liquid + β-Y ↔ $\gamma^{Mg\text{-}Y}$ + cph-Y	771.4	U_7	10.1	34.7	55.2
15	Liquid + AlY_2 ↔ Al_2Y_3 + cph-Y	908.7	U_8	23	8	69
16	Al_2Y + τ ↔ Liquid + Al_3Y	531.6	P	51.4	43	5.6

$$(Al\%, Mg, Y)_9: (Al, Mg\%, Y)_{1.6}: (Mg, Y\%)_{1.4}$$

This model gives good agreement with the primary solidification region obtained by Odinaev and Ganiev[11] and provides homogeneity in the composition range of $0 \leq X_{Al} \leq 0.877$, $0 \leq X_Y \leq 1$, and $0 \leq X_{Mg} \leq 1$, which covers the Al_4MgY compound. Based on the established model for τ-phase, the optimized parameters are listed in Table 5. Three *G* and one *L* parameters were used to reproduce the experimental primary solidification region of τ-phase.

To obtain better agreement with the experimental liquidus isotherms, two ternary interaction terms were added to the description of the liquid phase. These parameters are listed in Table 5. The resulting ternary phase diagram in comparison with the experimental results from the literature is shown in Fig. 6.

The ternary phase diagram of the Mg-Al-Y system was obtained in detail by projecting liquidus lines from isothermal sections at 100 °C temperature step on the Gibbs triangle. In this system, 16 ternary four-phase-equilibria points are determined: seven ternary eutectic points, eight ternary quasi peritectic points, and one ternary peritectic point (Table 6). Moreover, it involves fifteen ternary three-phase-equilibria points: eight saddle points, and seven binary eutectic points (Table 7). Also, good agreement can be seen in Fig. 6 between the calculated isothermal lines and the experimental values from the literature.

The calculated primary solidification region for the τ-phase shows good agreement with the report of Odinaev and Ganiev.[11] However, the calculated melting point of this compound is 1085 °C, which is much higher than ~780 °C obtained by Odinaev and Ganiev.[11] This contradiction is due to the fact that the liquidus around τ-phase was predicted to be higher than what reported by Odinaev and Ganiev.[11] Such a low liquidus in this region is very difficult to reproduce due to the high enthalpies and quite

Table 7 Calculated three-phase equilibria points and their reactions in the Al-Mg-Y system

No.	Reaction	Calculated invariant points				
				Composition, at.%		
		T, °C	Type	Al	Mg	Y
1	Liquid ↔ τ + fcc-Al	613.9	S_1	92.6	3.8	3.6
2	Liquid ↔ Al_2Y + τ	1088.6	S_2	75	10	15
3	Liquid ↔ $Al_{140}Mg_{89}$ + τ	432	S_3	63.5	34.3	2.2
4	Liquid ↔ τ + $\gamma^{Mg\text{-}Y}$	439.3	S_4	54.8	42.4	2.8
5	Liquid ↔ Al_2Y + cph-Mg	625	S_6	3.8	94.9	1.3
6	Liquid ↔ Al_2Y + ε	547.6	S_8	8.2	74.3	17.5
7	Liquid ↔ ε + AlY	549.8	S_9	10.4	66	23.6
8	Liquid ↔ Al_2Y_3 + $\gamma^{Mg\text{-}Y}$	730.7	S_{10}	13.3	34	52.7
9	Liquid ↔ AlY_2 + cph-Y	967.3	e_1	26	0	74
10	Liquid ↔ AlY + Al_2Y_3	1087.4	e_2	43	0	57
11	Liquid ↔ Al-fcc + Al_3Y	640	e_3	97.5	0	2.5
12	Liquid ↔ fcc-Al + $Al_{140}Mg_{89}$	449.3	e_4	63.8	36.2	0
13	Liquid ↔ $Al_{140}Mg_{89}$ + $\gamma^{Mg\text{-}Y}$	450	e_5	59.6	40.4	0
14	Liquid ↔ $\gamma^{Mg\text{-}Y}$ + cph-Mg	430.3	e_6	31.7	68.3	0
15	Liquid ↔ cph-Mg + ε	558.4	e_7	0	91.6	8.4

normal entropies of formation of the binary Al-Y intermetallic phases Al_3Y, Al_2Y, AlY, Al_2Y_3, and AlY_2. These high liquidus temperatures were observed by other researchers who studied similar systems (i.e., Mg-Al-RE).[56-58] Further, the existence of Al_4Y, not included in this work but considered by Odinaev and Ganiev,[11] may have contributed to this inconsistency. It is worth emphasizing that the most recent work[14,15,19] on Al-Y did not consider Al_4Y to be a stable phase in this system. Moreover, it is difficult to compare the calculated invariant reactions in this work with those of Odinaev and Ganiev[11] due to their acceptance

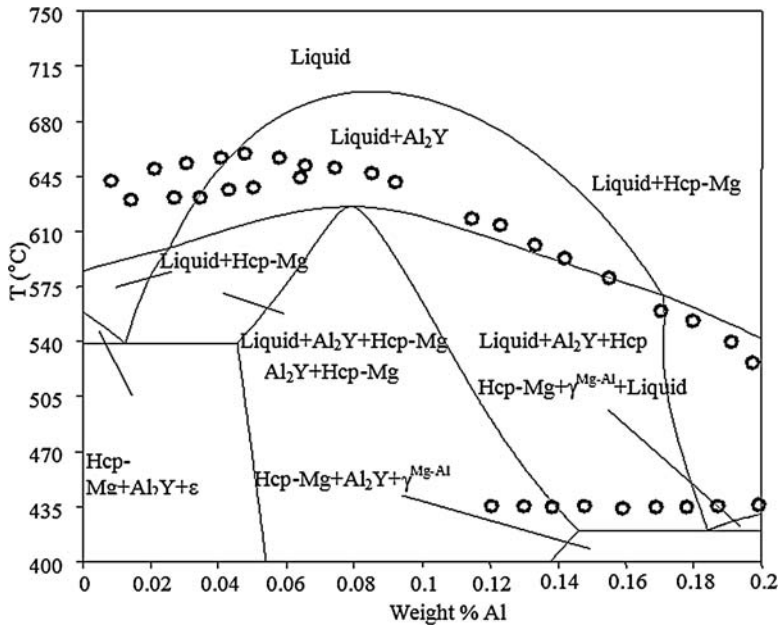

Fig. 7 Calculated vertical sections for 80 wt.% Mg compared with experimental data, 0-20 wt.% Al[47]

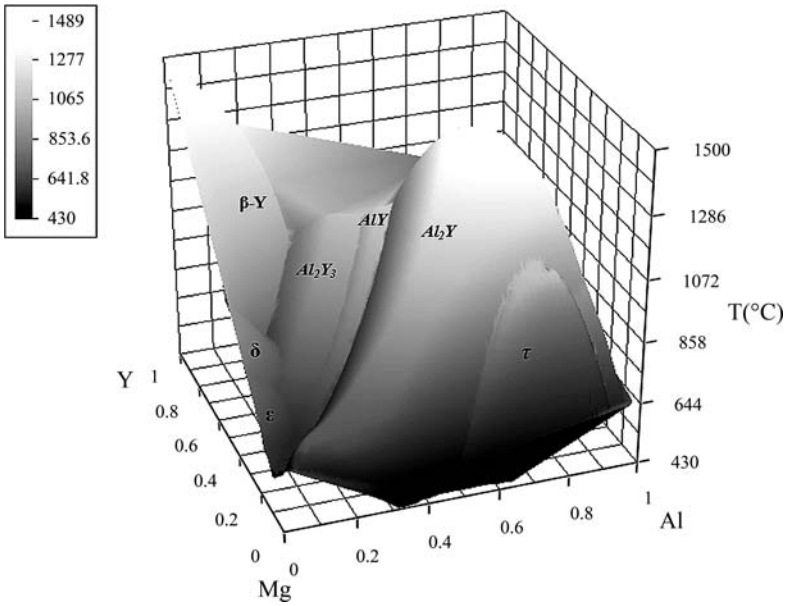

Fig. 8 Liquidus surface of the Al-Mg-Y system in 3D with color key indicating the temperature range

of Al_4Y. Nevertheless, reasonable agreement has also been achieved with the experimental work of Drits et al.[47] (Fig. 7). Figure 7 shows that the experimental data of Drits et al.[47] have boundaries at higher temperatures than those calculated, especially in the regions where the ε-phase exists. This is due to the high melting point of ε-phase (633 °C) reported by Drits et al.[47] However, this was evaluated as 614 °C in the current work, which is in good agreement with Smith et al.[38]

For a better understanding, the ternary Al-Mg-Y liquidus surface is drawn in three dimensions, with the temperature color key, from the evaluated thermodynamic model using GRAPHIS software[59] (Fig. 8). The light grey color expresses the high-temperature range, and the dark gray presents the low-temperature range, as shown in the legend of this figure.

5. Conclusions

The phase relations and thermodynamic descriptions of the Al-Y and Mg-Y systems were obtained using optimiza-

tion with the phase equilibria and thermodynamic experimental data from the literature. A consistent set of thermodynamic parameters were obtained in this work. These parameters were used to calculate the Mg-Al-Y phase diagram. The calculated results were compared with the experimental data, and good agreement has been achieved.

One ternary nonstoichiometric compound was included in the assessment of the Mg-Al-Y ternary system. The Gibbs energy of this ternary compound was evaluated using a sublattice model, and to obtain good agreement with the experimental liquidus isotherms, two ternary interaction parameters were added to the description of the liquid phase.

Good agreement with the experimental data has been achieved for the calculated binary systems and for the thermodynamic properties of the binary phases. This was extended to calculate liquidus isotherms, the primary solidification region of τ-phase, and a vertical section for the ternary Mg-Al-Y system.

The predicted invariant points in the Mg-Al-Y system were sixteen ternary-four phase equilibria points: seven ternary eutectic points, eight ternary quasi peritectic points, and one ternary peritectic point. Further, fifteen ternary-three phase equilibria points were determined: eight saddle points and seven binary eutectic points.

Acknowledgments

The authors gratefully acknowledge financial support from HQSF, Hani Qaddumi Scholarship Foundation-Jordan and Natural Science and Engineering Research Council of Canada (NSERC), Canada through the Discovery Grant Program.

References

1. J. Gröbner, D. Kevorkov, R. Schmid-Fetzer, F.W. Bach, H. Haferkamp, and C. Jaschik, The CALPHAD Approach in the Focused Design of Magnesium Alloy, J.-C. Zhao, M. Fahrmann, and T. Pollock, Ed., *Materials Design Approaches and Experiences,* TMS, 2001, p 241-253
2. M. Suzuki, H. Sato, K. Maruyama, and H. Oikawa, Creep Behavior and Deformation Microstructures of Mg–Y alloys at 550 K, *Mater. Sci. Eng. A,* **252**(2), 1998, p 248-255
3. I.A. Anyanwu, S. Kamado, and Y. Kojima, Aging Characteristics and High Temperature Tensile Properties of Mg-Gd-Y-Zr Alloys, *Mater. Sci. Eng. A,* 2001, **42**(7), p 1206-1211
4. H. Seifert, J. Gröbner, F. Aldinger, F.H. Hayes, G. Effenberg, C. Batzner, H. Flandorfer, P. Rogl, A. Saccone, and R. Ferro, Thermodynamic Calculation and Experimental Studies of Phase Relations in the Mg-Mn-Y-Zr System, B.W. Lorimer, Ed., *Proceedings of the International Magnesium Conference,* 3rd ed. Apr. 10-12, 1996 (Manchester, UK), Institute of Materials, London, UK, 1997, p 257-270
5. N.V. Ravi Kumar, J.J. Blandin, M. Suery, and E. Grosjean, Effect of Alloying Elements on the Ignition Resistance of Magnesium Alloys, *Scripta Mater.,* 2003, **49,** p 225-230
6. M. Socjusz-Podosek and L. Lity nska, Effect of Yttrium on Structure and Mechanical Properties of Mg Alloys, *Mater. Chem. Phys.,* 2003, **80**(2), p 472-475
7. I. Ansara, A.T. Dinsdale, and M.H. Rand, COST507–Thermochemical Database for Light Metal Alloys, European Commission EUR 18499, Brussels, 1998
8. A. Dinsdale, SGTE Data for Pure Elements, *CALPHAD,* 1991, **15**(4), p 317-425
9. O. Redlich, A.T. Kister, Thermodynamics of Nonelectrolyte Solutions, X-Y-T Relations in a Binary System, *J. Ind. Eng. Chem.,* 1948, **40**, p 341-345
10. Pandat 4.0: Multi-Component Phase Diagram Calculation Software, Computherm LLC, Madison, WI, 2000-2003
11. Kh.O. Odinaev and I.N. Ganiev, Quasibinary Sections and Liquidus Surface of the Aluminum-Magnesium-Yttrium Aluminide (YAl_2) System, *Izv. Vyssh. Uchebn. Zaved. Tsvetn, Metall.,* 1990, **6,** p 90-95, in Russian
12. K.C. Hari Kumar and P. Wollants, Some Guidelines for Thermodynamic Optimization of Phase Diagrams, *J. Alloys Compd.,* 2001, **320**(2), p 189-198
13. E.M. Savitskii and V.F. Terekhova, Study of Rare Metals and Alloys, E.M. Savitski, Ed., *IP Bardin Razvit. Metall. SSSR,* Moscow, USSSR Conference, Nauka, Moscow, 1976, p 240-57, in Russian
14. R.L. Snyder, "Yttrium-Aluminum Alloy Studies," Master's Thesis, Iowa State University for Science and Technology, Ames, IA, 1960
15. C.E. Lundin, Jr. and D.T. Klodt, Phase Equilibria in The Yttrium-Aluminum System, *Am. Soc. Metals Trans. Quart.,* 1961, **54**(2), p 68-75
16. M.E. Drits, E.S. Kadaner, and N.D. Shoa, Structure and Properties of Aluminum-Rich Al-Y Alloys, *Izv. Akad, Nauk SSSR, Metally,* 1969, **6,** p 150-153, in Russian
17. K.A. Gschneidner, Jr. and F.W. Calderwood, The Al-Y (Aluminum-Yttrium) System, Ames Lab., Iowa State Univ., Ames, IA, USA, *Bull. Alloy Phase Diagrams,* 1989, **10**(1), p 44-47
18. P.I. Kripyakevich, The Crystal Structure of YAl_2, *Kristallografiya,* 1960, **5,** p 463-464
19. C. Rongzhen, W. Xiangzhong, and L. Jingqi, The Isothermal Section of the Phase Diagram of the Ternary System Al-Sn-Y at Room Temperature, *J. Alloys Compd.,* 1995, **218**(2), p 221-223
20. Z. Lingmin and W. Shouyu, The 800 K Isothermal Section of the Y-Al-Sb Phase Diagram, *J. Alloys Compd.,* 2003, **351**(1-2), p 176-179
21. A. Chelkowski, E. Talik, J. Szade, J. Heimann, A. Winiarska, and A. Winiarski, Solid Solubility of Rare Earths in Aluminum, *J. Less-Common Met.,* 1988, **141**(2), p 213-216
22. R. Richter, Z. Altounian, J.O. Strom-Olsen, U. Koester, and M. Blank-Bewersdorff, Y_5Al_3, A New Yttrium-Aluminum Compound, *J. Mater. Res.,* 1987, **22**(8), p 2983-2986
23. D.M. Bailey, Structures of Two Polymorphic Forms of YAl_3, *Acta Crystallogr.,* 1967, **23**(5), p 729-733
24. R. Raggio, G. Borzone, and R. Ferro, The Al-Rich Region in the Y-Ni-Al System: Microstructures and Phase Equilibria, *Intermetallics,* 2000, **8**(3), p 247-257
25. Yu.O. Esin, P.V. Gel'd, M.S. Petrushevskii, G.M. Ryss, and A.I. Stroganov, Enthalpies of Formation of Yttrium and Aluminum Melts. *Doklady Akademii Nauk SSSR,* 1976, **228**(2), p 386-388, in Russian, [English translation available at: *Doklady Phys. Chem.,* 1976, **228**(2), p 458-460]
26. G.M. Ryss, Yu.O. Esin, and A.I. Stroganov, and P.V. Gel'd, Enthalpies of Formation of Yttrium- Aluminum Molten Alloys, *Zh. Fiz. Khim,* 1976, **50**(4), p 985-986, in Russian
27. V.I. Kober, I.F. Nichkov, S.P. Raspopin, and V.N. Nauman, Phase Composition and Thermodynamic Properties of Yttrium-Aluminum System, *Izv. Vyssh. Uchebn. Zaved., Tsvetn, Metall.,* 1979, **5,** p 40-43, in Russian
28. G.N. Zviadadze, A.A. Petrov, and E.K. Kazenas, Thermodynamics of the Vacuum Evaporation of Alloys of Scandium,

Yttrium, Lanthanum, and Neodymium with Aluminum, A.I. Monokhin, Ed., *Protsessy Tsvetnoei Metallurgii pri Nizkikh Davleniyakh,* Izd. Nauka, Moscow, USSR, 1983, p 94-98, in Russian
29. J. Gröbner, H. Lukas, and F. Aldinger, Thermodynamic Calculations in the Y-Al-C System, *J. Alloys Compd.,* 1995, **220**(1-2), p 8-14
30. V.S. Timofeev, A.A. Turchanin, A.A. Zubko, Vl, and I.A. Tomilin, Enthalpies of Formation for the Al-Y and Al-Y-Ni Intermetallic Compounds, *Thermochim. Acta,* 1997, **299,** p 37-41, in Russian
31. G. Borzone, A. Cicciolia, P.L. Cigninia, M. Ferrinia, and D. Gozzia, Thermodynamics of the YA1-YAl_2 System, *Intermetallics,* 2000, **8**(3), p 203-212
32. M.S. Petrusheveskii and G.M. Ryss, Calculations of the Activities of Components in Liquid Binary Alloys of Yttrium with Aluminum and Silicon, *Zh. Fiz. Khim.,* 1986, **60**(6), p 1532-1535, in Russian
33. V.K. Kulifeev and V.N. Kaplenkov, Thermodynamics of the Interaction in the System Yttrium-Aluminum, *Zh. Metall.,* 1981, **131,** p 110-112, in Russian
34. Z.A. Sviderskaya and E.M. Padezhnova, Phase Equilibriums in Magnesium-Yttrium and Magnesium-Yttrium-Manganese Systems, *Izv. Akad. Nauk. SSSR Metally,* 1968, **6,** p 183-190, in Russian
35. E.D. Gibson and O.N. Carlson, The Yttrium-Magnesium Alloy System, *Trans. Am. Soc. Metal.,* 1960, **52,** p 1084-1096
36. D. Mizer and J.B. Clark, Magnesium-Rich Region of the Magnesium-Yttrium Phase Diagram, *T. Am. I. Min. Met. Eng.,* 1961, **221,** p 207-208
37. T.B. Massalski, *Binary Alloy Phase Diagrams,* 2nd Ed., ASM International, 1990, p 1-3
38. J.F. Smith, D.M. Bailey, D.B. Novotny, and J.E. Davison, Thermodynamics of Formation of Yttrium-Magnesium Intermediate Phases, *Acta Mater.,* 1965, **13**(8), p 889-895
39. H. Flandorfer, M. Giovannini, A. Saccone, P. Rogl, and R. Ferro, The Ce-Mg-Y System, *Metall. Mater. Trans. A,* 1997, **28A**(2), p 265-276
40. M.-X. Zhang and P.M. Kelly, Edge-to-edge Matching and Its Applications Part II. Application to Mg-Al, Mg-Y, and Mg-Mn Alloys, *Acta Mater.,* 2005, **53**(4), p 1085-1096
41. R. Agarwal, H. Feufel, and F. Sommer, Calorimetric Measurements of Liquid La-Mg, Mg-Yb, and Mg-Y Alloys, *J. Alloys Compd.,* 1995, **217**(1), p 59-64
42. O.B. Fabrichnaya, H.L. Lukas, G. Effenberg, and F. Aldinger, Thermodynamic Optimization in the Mg-Y System, *Intermetallics,* 2000, **11**(11-12), p 1183-1188
43. V. Ganesan, F. Schuller, F. Harald, F. Sommer, and H. Ipser, Thermodynamic Properties of Ternary Liquid Cu-Mg-Y Alloys, *Z. MetaIlkd.,* 1997, **88**(9), p 701-710
44. V. Ganesan and H. Ipser, Thermodynamic Properties of Liquid Magnesium-Yttrium Alloys, *J. Chim. Physique.,* 1997, **94**(5), p 986-991
45. Q. Ran, H.L. Lukas, G. Effenberg, and G. Petzow, Thermodynamic Optimization of the Magnesium-Yttrium System, *CALPHAD,* 1988, **12**(4), p 375-381
46. I.N. Pyagai, E.Z. Khasanova, A.V. Vakhobov, and O.V. Zhikhareva, Heat of Formation of the Intermetallic Compound Magnesium Ytterbium (Mg_2Yb) at 298 K, *Dokl. Akad. Nauk Tadzh. SSR.,* 1990, **33**(9), p 602-604
47. M.E. Drits, E.M. Padezhnova, and T.V. Dobatkina, Phase Equilibriums in Magnesium-Yttrium-Aluminum Alloys, *Izv. Akad. Nauk. SSSR Metally,* 1979, **3,** p 223-227
48. O.S. Zarechnyuk, M.E. Drits, R.M. Rykhal, and V.V. Kinzhibalo,Study of a Magnesium-Aluminum-Yttrium System at 400 in the Phase Containing 0-33.3 at.% Yttrium, *Izv. Akad. Nauk. SSSR Metally,* 1980, **5,** p 242-244
49. Kh.O. Odinaev, I.N. Ganiev, V.V. Kinzhibalo, and Kh.K. Kurbanov, Phase Equilibria in Aluminum-Magnesium-Yttrium and Aluminum-Magnesium-Cerium Systems at 673 K, *Izv. Vyssh. Uchebn. Zaved. Chern, Metall.,* 1989, **4,** p 75-77, in Russian
50. Q. Ran, H.L. Lukas, G. Effenberg, and G. Petzow, A Thermodynamic Optimization of the Aluminum-Yttrium System, *J. Less-Common Met.,* 1989, **146,** p 213-222
51. S. Stølen, T. Grande, *Chemical Thermodynamics of Material Macroscopic and Microscopic Aspects,* John Wiley & Sons, New York, 2004.
52. A.R. Miedema, On the Heat of Formation of Solid Alloys, *J. Less-Common Met.,* 1976, **46**(1), p 67-83
53. K.C. Hari Kumar, I. Ansara, and P. Wollants, Sublattice Modeling of the μ-Phase, *CALPHAD,* 1998, **22**(3), p 323-334
54. P. Villars and L.D. Calvert, *Pearson Handbook of Crystallographic Data for Intermetallic Phases,* 2nd ed, ASM International, 1991
55. W. Kraus and G. Nolze, Powder Cell for Windows, Version 1.0, Federal Institute for Materials Research and Testing, Berlin, Germany, 1997
56. J. Gröbner, R. Schmid-Fetzer, A. Pisch, G. Cacciamani, P. Riani, and R. Ferro, Experimental Investigation and Thermodynamic Calculation of the Al-Mg-Sc System, *Z. Metallkd.,* 1999, **90**(11), p 872-880
57. J. Gröbner, D. Kervokov, and R. Schmid-Fetzer, Thermodynamic of Al-Gd-Mg Phase Equilibria Checked by Key Experiments, *Z. Metallkd.,* 2001, **92**(1), p 2-7
58. J. Gröbner, D. Kervokov, and R. Schmid-Fetzer, Thermodynamic modeling of Al-Ce-Mg Phase Equilibria Coupled with Key Experiments, *Intermetallics,* 2002, **10**(5), p 415-422
59. Graphis Graphing Software for 2D and 3D Data—High-Quality Scientific/Engineering Visualization for the Windows DesktopA, Version: 2.6.2, Kylebank Software Ltd., Ayr, UK, 2003